HUMming to the MUSIC

On the use of control methods for imaging small imperfections

Mark Asch

Université d'Amiens (LAMFA UMR-CNRS 6140)
Université libre de Bruxelles (Environmental Hydroacoustics Lab)

December 2nd, 2011

Joint work with...

- *Habib Ammari*, Ecole Normale Supérieure, Paris.
- *Vincent Jugnon*, Ecole Polytechnique, Palaiseau.
- *Marion Darbas, Jean-Baptiste Duval,* Amiens.

Convergence of 2 ideas

Convergence of 2 ideas

HUM: Controllability of the wave equation

Convergence of 2 ideas

HUM: Controllability of the wave equation

MUSIC: Imaging algorithms for small-volume imperfections.

Convergence of 2 ideas

HUM: Controllability of the wave equation

MUSIC: Imaging algorithms for small-volume imperfections.

Result

We can perform transient imaging with limited-view data, using waves as probes and employing practical imaging techniques

Convergence of 2 ideas

HUM: Controllability of the wave equation

MUSIC: Imaging algorithms for small-volume imperfections.

Result

We can perform transient imaging with limited-view data, using waves as probes and employing practical imaging techniques

Key reference

H. Ammari, *An inverse IBVP for the wave equation in the presence of imperfections of small volume, SICON* ***41****, 4 (2002).*

Outline

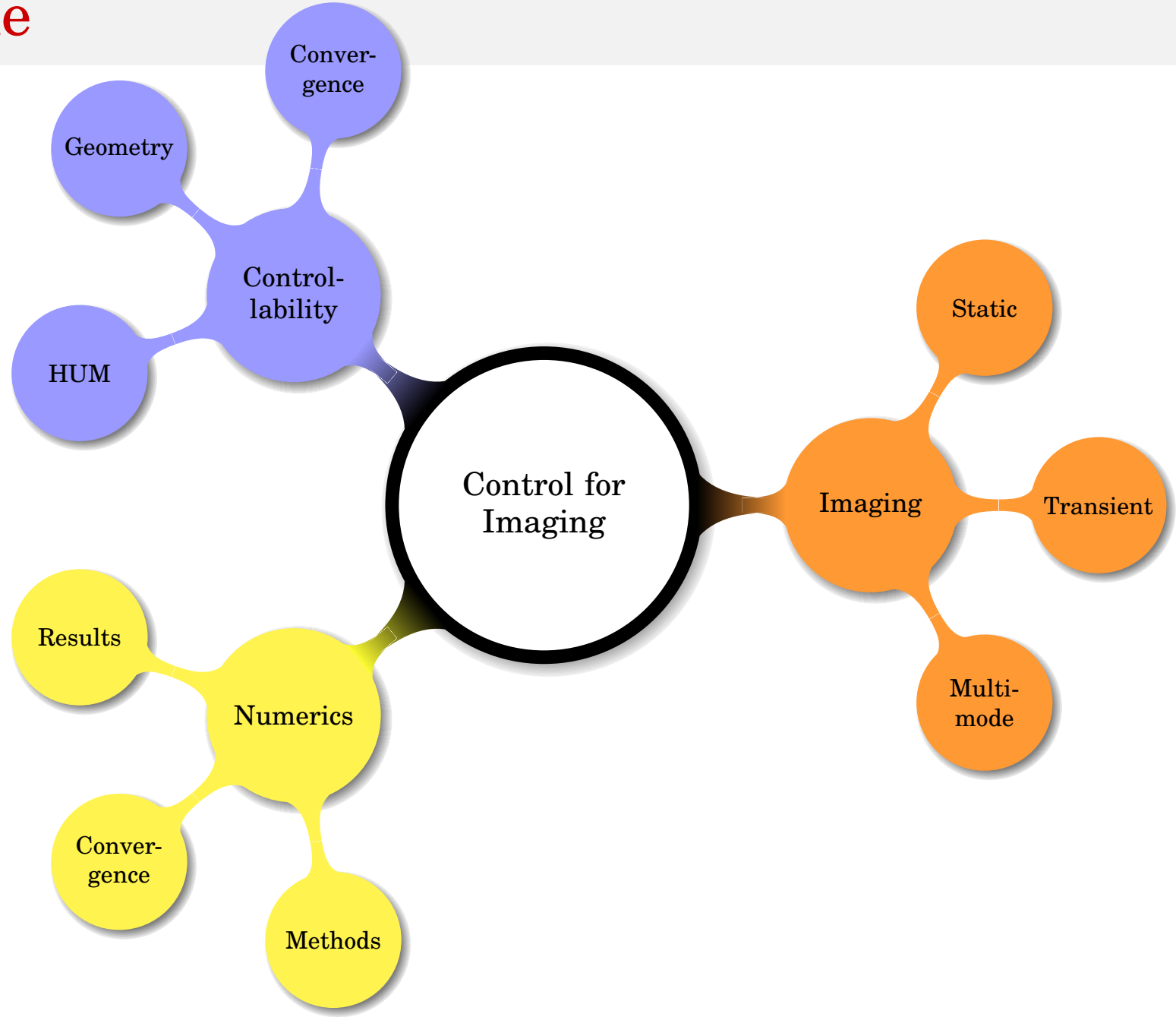
Control for Imaging
Control-lability
Geometry
Conver-gence
HUM
Imaging
Static
Transient
Multi-mode
Numerics
Results
Conver-gence
Methods

Contents

Contents

Formulation of exact controllability

The wave equation with Dirichlet control:

$$\left(\partial_t^2 - c^2\Delta\right) u = 0 \qquad \text{in } \Omega \times (0,T)\,,$$

$$u|_{t=0} = u^0,\ \partial_t u|_{t=0} = u^1 \qquad \text{in } \Omega, \tag{1}$$

$$u = \begin{cases} g & \text{on } \Gamma_c \times (0,T), \\ 0 & \text{on } \Gamma \setminus \Gamma_c \times (0,T), \end{cases}$$

Formulation of exact controllability

The wave equation with Dirichlet control:

$$\left(\partial_t^2 - c^2\Delta\right) u = 0 \qquad \text{in } \Omega \times (0,T)\,,$$

$$u|_{t=0} = u^0,\ \partial_t u|_{t=0} = u^1 \qquad \text{in } \Omega, \tag{1}$$

$$u = \begin{cases} g & \text{on } \Gamma_c \times (0,T), \\ 0 & \text{on } \Gamma \setminus \Gamma_c \times (0,T), \end{cases}$$

- Geometry and control time: T

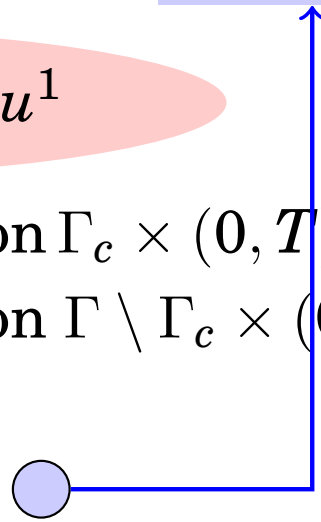

Formulation of exact controllability

The wave equation with Dirichlet control:

$$\left(\partial_t^2 - c^2\Delta\right) u = 0 \qquad \text{in } \Omega \times (0,T)\,,$$

$$u|_{t=0} = u^0,\ \partial_t u|_{t=0} = u^1 \qquad \text{in } \Omega, \tag{1}$$

$$u = \begin{cases} g & \text{on } \Gamma_c \times (0,T), \\ 0 & \text{on } \Gamma \setminus \Gamma_c \times (0,T), \end{cases}$$

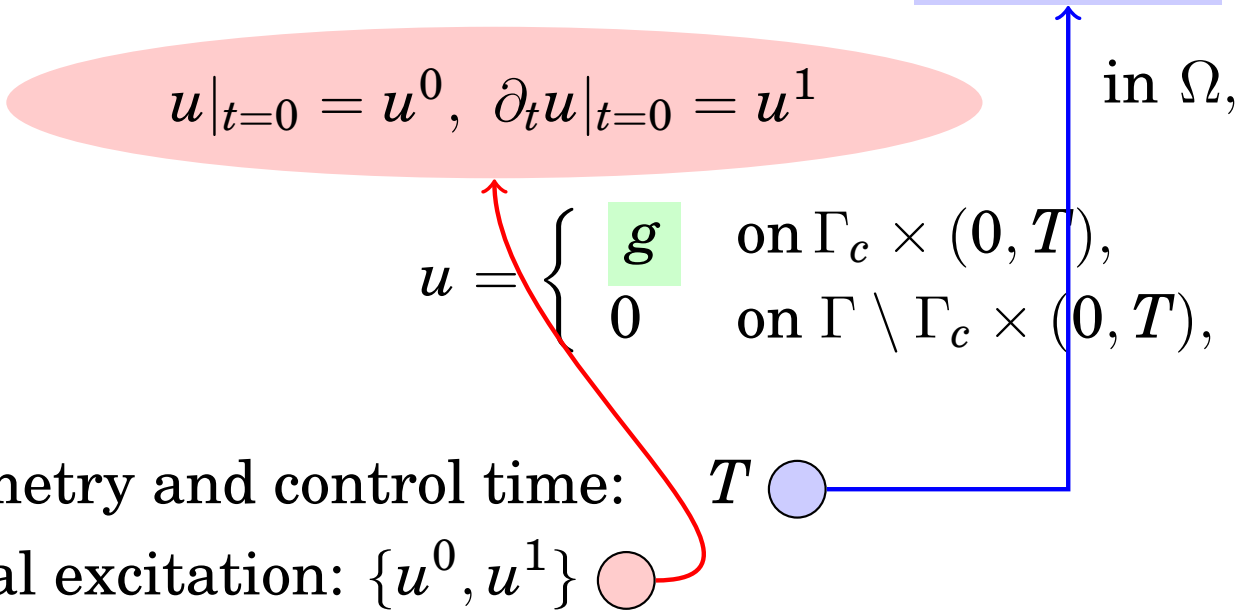

- Geometry and control time:
- Initial excitation: $\{u^0, u^1\}$

Formulation of exact controllability

The wave equation with Dirichlet control:

$$\left(\partial_t^2 - c^2\Delta\right) u = 0 \qquad \text{in } \Omega \times (0,T)\,,$$

$$u|_{t=0} = u^0,\ \partial_t u|_{t=0} = u^1 \qquad \text{in } \Omega, \tag{1}$$

$$u = \begin{cases} g & \text{on } \Gamma_c \times (0,T), \\ 0 & \text{on } \Gamma \setminus \Gamma_c \times (0,T), \end{cases}$$

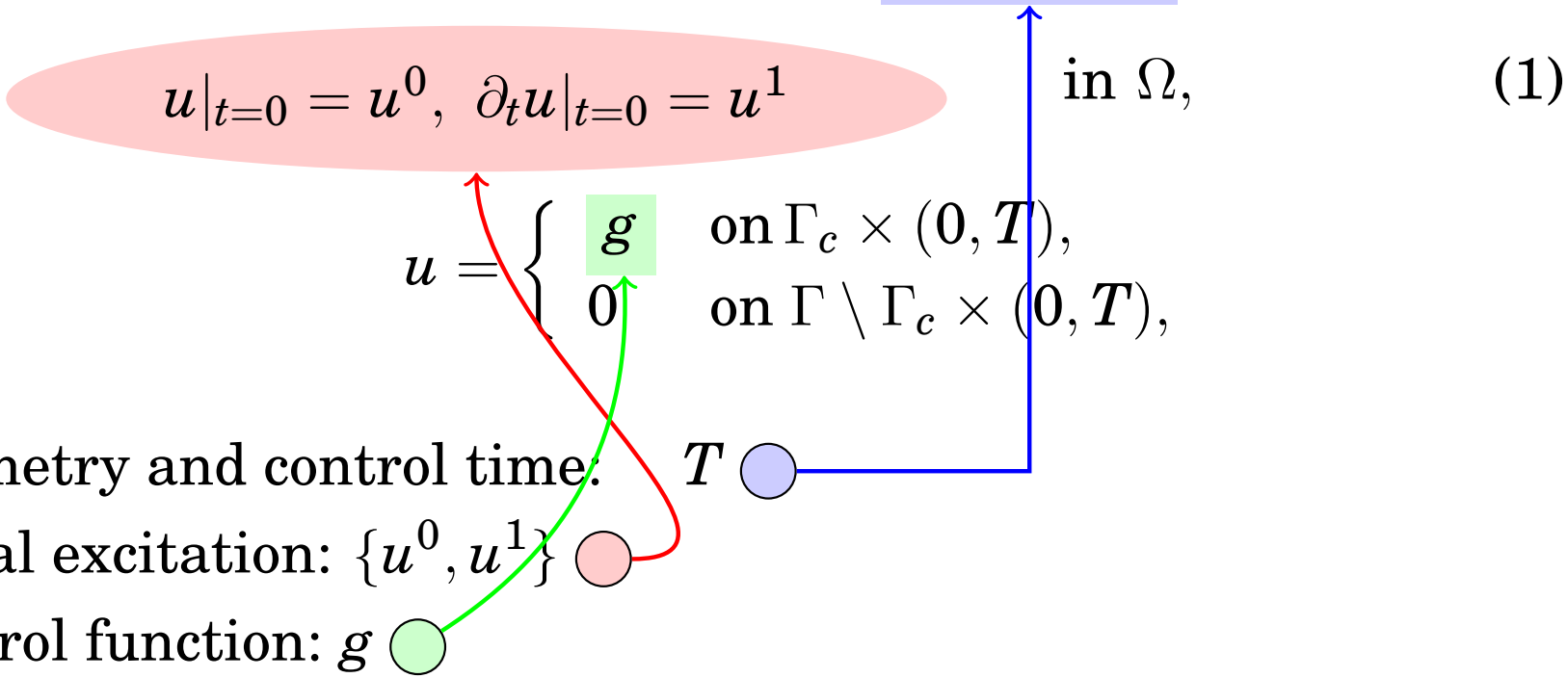

- Geometry and control time: T
- Initial excitation: $\{u^0, u^1\}$
- Control function: g

Existence and uniqueness of g by the HUM

The problem of exact boundary controllability:

"Given T, u^0, u^1, find a control g such that the solution of (1) satisfies, at time T,

$$u(x,T) = \partial_t u(x,T) = 0 \ \text{ in } \Omega"$$

Existence and uniqueness of g by the HUM

The problem of exact boundary controllability:

"Given T, u^0, u^1, find a control g such that the solution of (1) satisfies, at time T,

$$u(x,T) = \partial_t u(x,T) = 0 \ \text{ in } \Omega"$$

Theorem [Lions'88]

For T large enough, there exists a unique control g that minimizes the $L^2(\Gamma_c \times (0,T))$ norm. This control can be constructed by the Hilbert Uniqueness Method.

Existence and uniqueness of g by the HUM

The problem of exact boundary controllability:

"Given T, u^0, u^1, find a control g such that the solution of (1) satisfies, at time T,

$$u(x,T) = \partial_t u(x,T) = 0 \ \text{ in } \Omega"$$

Theorem [Lions'88]

For T large enough, there exists a unique control g that minimizes the $L^2(\Gamma_c \times (0,T))$ norm. This control can be constructed by the Hilbert Uniqueness Method.

Proof.

(constructive...) Set up the optimality system: equation (forward) plus adjoint (backward). Then show the invertibility of the HUM operator $\Lambda \boldsymbol{e} = \boldsymbol{f}$, where $\boldsymbol{e}$ is the initial condition of the forward equation and $\boldsymbol{f}$ is the final condition of the backward equation. Finally, compute g by a preconditioned, conjugate gradient algorithm.

Geometric controllability

GCC [Bardos, Lebeau, Rauch - SICON'92]

Every ray of geometrical optics, starting at any point $x \in \Omega$, at time $t = 0$, hits Γ_c before time T at a nondiffractive point.

Geometric controllability

GCC [Bardos, Lebeau, Rauch - SICON'92]

Every ray of geometrical optics, starting at any point $x \in \Omega$, at time $t = 0$, hits Γ_c before time T at a nondiffractive point.

- No "glancing" nor "trapped" rays.

Geometric controllability

GCC [Bardos, Lebeau, Rauch - SICON'92]

Every ray of geometrical optics, starting at any point $x \in \Omega$, at time $t = 0$, hits Γ_c before time T at a nondiffractive point.

- No "glancing" nor "trapped" rays.

Uncontrollable and controllable geometries

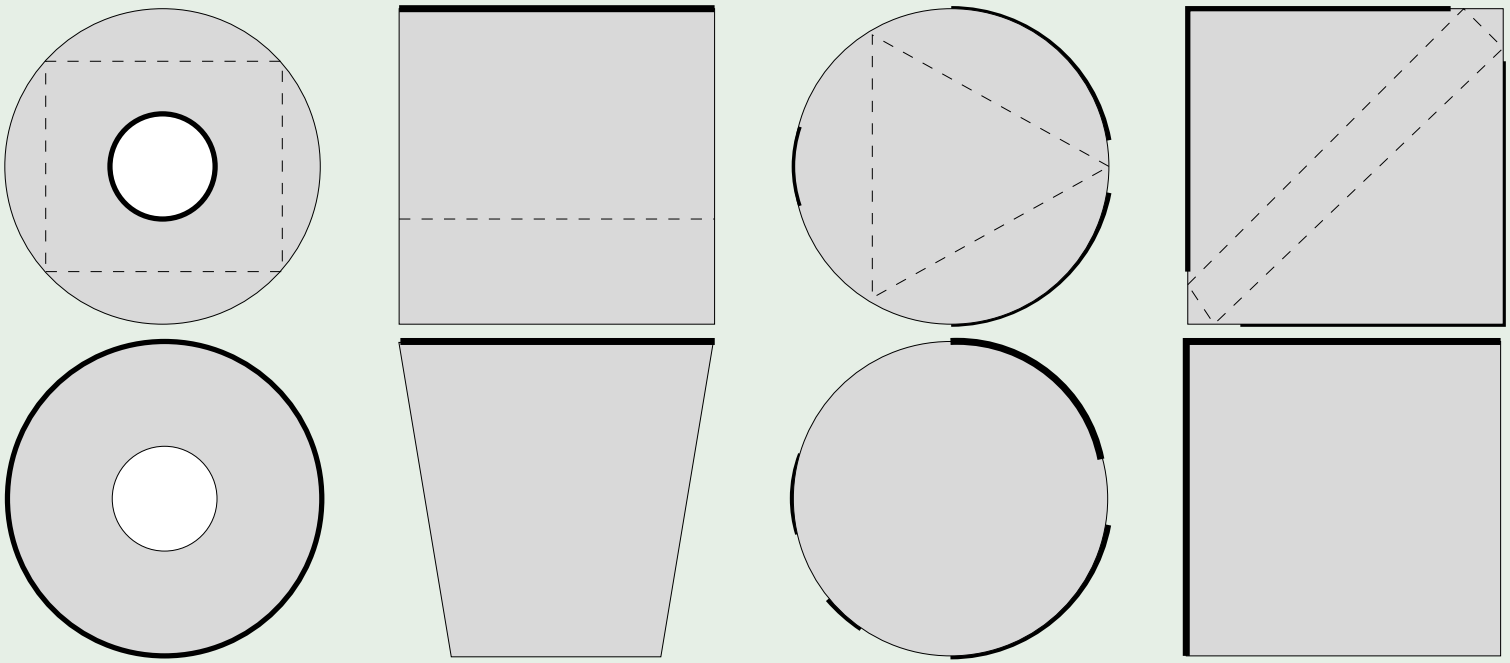

So where's the catch?

So where's the catch?

- Numerically, the HUM produces an ill-posed problem...

Ill-posedness

$$\text{stability} + \text{consistency} \not\Rightarrow \text{convergence}$$

So where's the catch?

- Numerically, the HUM produces an ill-posed problem...

Ill-posedness

$$\text{stability} + \text{consistency} \not\Rightarrow \text{convergence}$$

- Various solutions:
  - Tykhonov regularization.
  - Mixed finite elements.
  - Bi-grid filtering.
  - Uniformly controllable schemes.
  - Spectral approach.

Contents

Convergence

What is known?

- 1D
- 2D in a periodic region
- finite differences in space and time
- **structured** finite-element meshes

What is still to be done?

General, unstructured finite-element meshes on arbitrary geometries.

Two possible approaches:

- "analytical" approach based on observability estimations;
- "numerical analysis" approach based on finite-element convergence estimations.

Contents

Contents

Electrical Impedance Imaging

Simplest example that contains ALL the ingredients...

Idea:

Impose (a finite number of) boundary voltages and measure the induced boundary currents to estimate the electrical conductivity.

Electrical Impedance Imaging

Simplest example that contains ALL the ingredients...

Idea:

Impose (a finite number of) boundary voltages and measure the induced boundary currents to estimate the electrical conductivity.

Asymptotic approach:

Use outer expansions in terms of the characteristic size of the anomaly.

Identification of small-volume imperfections

Formulation

- $\Omega \subset \mathbf{R}^d$, $d = 2, 3$: bounded, Lipschitz domain, u background solution of the homogeneous equation

$$\begin{cases} \Delta u = 0 \quad \text{in } \Omega, \\ k_0 \ \frac{\partial u}{\partial \nu}\big|_{\partial\Omega} = g \end{cases} \tag{2}$$

  where $g \in L^2_0(\partial\Omega) = \{g \in L^2(\partial\Omega), \int_{\partial\Omega} g \, d\sigma = 0\}$.
- m small inclusions, $D_s = z_s + \epsilon B_s$ pairwise-separated and boundary-separated, centres z_s, size ϵ, shapes B_s (Lipschitz), conductivities $k_s \neq k_0$ for $1 \leq s \leq m$.
- u_ϵ voltage potential, solution of the perturbed equation

$$\begin{cases} \nabla \cdot \left(k_0 \chi\left(\Omega \setminus \bigcup_{s=1}^m \overline{D_s}\right) + \sum_{s=1}^m k_s \chi(D_s) \right) \nabla u_\epsilon = 0 \quad \text{in } \Omega, \\ k_0 \ \frac{\partial u_\epsilon}{\partial \nu}\big|_{\partial\Omega} = g. \end{cases} \tag{3}$$

Asymptotic expansion for $u_\epsilon - u$

$$(u_\epsilon - u)(y) = -\epsilon^d \sum_{s=1}^{m} \left(\frac{k_0}{k_s} - 1 \right) \nabla_x N(z_s, y) \cdot M^{(s)} \nabla u(z_s) + o(\epsilon^d) \quad (4)$$

[Friedman, Vogelius, *ARMA*, 1989]

- $N(x,y)$ is the Neumann function

$$\begin{cases} \Delta_x N(x,y) = -\delta_y & \text{dans } \Omega, \\ \left. \frac{\partial N}{\partial \nu_x} \right|_{\partial\Omega} = -\frac{1}{|\partial\Omega|} \end{cases}$$

- $M^{(s)}$ is a symmetric $d \times d$, polarization tensor,

$$M^{(s)}_{lm} = |B_s| \, \delta_{lm} - \int_{\partial B_s} \frac{k_0}{k_l} \frac{\partial \phi^+_m}{\partial \nu} \, d\sigma_y$$

- ϕ^+_m is a "corrector": harmonic inside and outside B, zero at ∞, with zero jumps across ∂B.

Inversion Methodology

- Apply the asymptotic formula in order to identify the location and certains properties of the shape of the imperfections.
- Using methods based on taking suitable averages of the boundary measurements using special background solutions as weights.
- The term of order ϵ^d corresponds physically to a voltage potential due to m polarized dipoles located at the points z_s, $1 \leq s \leq m$.

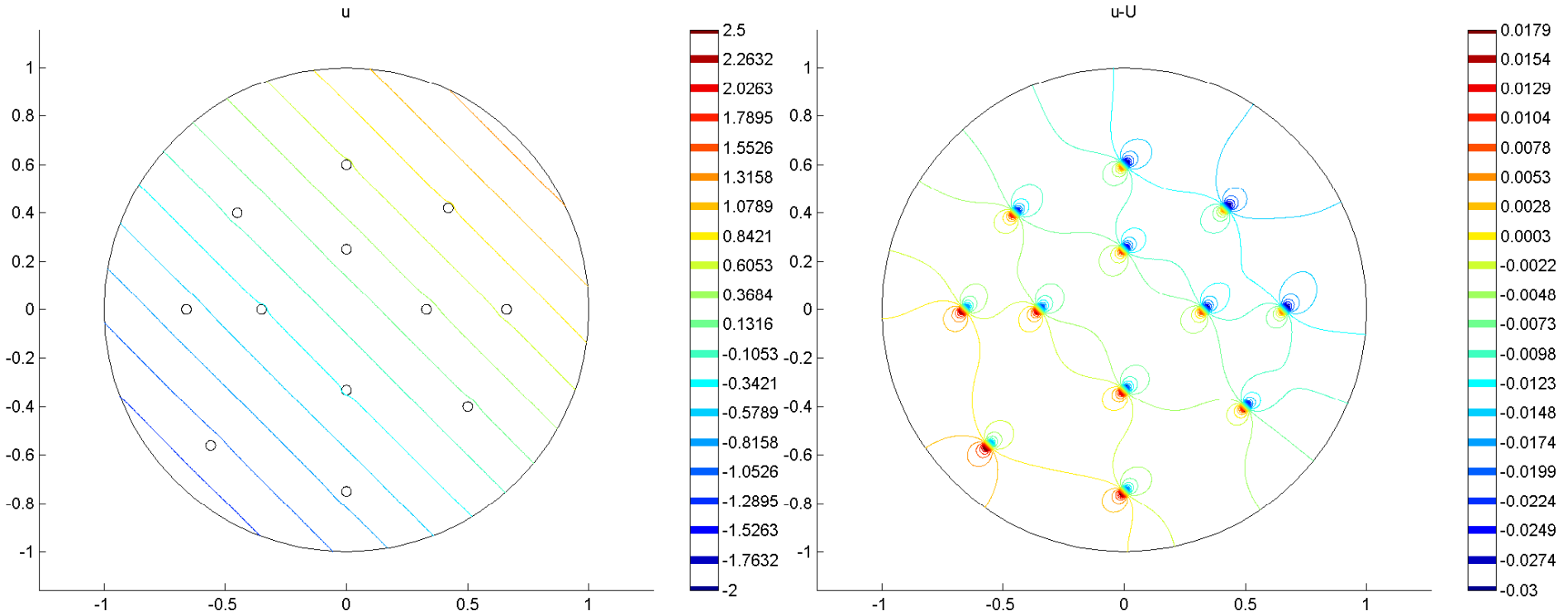

Numerous Algorithms

- Current projection Apply $(d =)2$ currents, $g_i = k_0 \nu_i$, corresponding to background potentials $u_i = x_i$, $i = 1, 2$; then use 2 (harmonic) test functions, $w_i = x_i$, $i = 1, 2$
- Fourier Inversion : for $\eta \in \mathbb{R}^2$ arbitrary, apply currents

$$g = i(\eta + i\eta^{\perp}) \cdot \nu e^{i(\eta + i\eta^{\perp}) \cdot x}$$

and test functions

$$w = e^{i(\eta + i\eta^{\perp}) \cdot x}$$

then $\Gamma(\eta)$ is the Fourier transformation of a linear combination of derivatives of delta functions centered at the points $2z_s$.

- Quadratic method.
- Least squares method.
- Linear sampling method.
- MUSIC method.
- Dynamical methods...

Contents

Acoustic wave equation

IBVP for the wave equation, in the *presence* of the imperfections,

$$(\mathrm{W}_\alpha)\begin{cases} \dfrac{\partial^2 u_\alpha}{\partial t^2} - \nabla\cdot(\gamma_\alpha \nabla u_\alpha) = 0 & \text{in } \Omega\times(0,T), \\ u_\alpha = f & \text{on } \partial\Omega\times(0,T), \\ u_\alpha|_{t=0} = u^0\ ,\ \left.\dfrac{\partial u_\alpha}{\partial t}\right|_{t=0} = u^1 & \text{in } \Omega. \end{cases}$$

Define u to be the solution in the *absence* of any imperfections,

$$(\mathrm{W}_0)\begin{cases} \dfrac{\partial^2 u}{\partial t^2} - \nabla\cdot(\gamma_0 \nabla u) = 0 & \text{in } \Omega\times(0,T), \\ u = f & \text{on } \partial\Omega\times(0,T), \\ u|_{t=0} = u^0\ ,\ \left.\dfrac{\partial u}{\partial t}\right|_{t=0} = u^1 & \text{in } \Omega. \end{cases}$$

Control function

- Suppose that T and the part Γ_c of the boundary $\partial\Omega$ are such that they geometrically control Ω.
- Then, for any $\eta \in \mathbb{R}^d$, we can construct by the Hilbert uniqueness method (HUM), a unique $g_\eta \in H_0^1(0,T;L^2(\Gamma))$ in such a way that the unique weak solution w_η of the wave equation

$$(\mathrm{W}_c)\begin{cases} \dfrac{\partial^2 w_\eta}{\partial t^2} - \nabla\cdot(\gamma_0\nabla w_\eta) = 0 & \text{in } \Omega\times(0,T), \\ w_\eta = g_\eta \text{ in } \Gamma_c\times(0,T), & w_\eta = 0 \text{ in } \partial\Omega\backslash\bar{\Gamma}_c\times(0,T), \\ w_\eta|_{t=0} = \beta(x)e^{i\eta\cdot x}\in H_0^1(\Omega), & \left.\dfrac{\partial w_\eta}{\partial t}\right|_{t=0} = 0 \text{ in } \Omega, \end{cases}$$

- satisfies $w_\eta(T) = \partial_t w_\eta(T) = 0$.

Key theorem (H. Ammari)

Theorem

Let $\eta \in \mathbb{R}^d$, $d = 2, 3$. Let u_α be the unique solution to the wave equation (W_α) with

$$u^0(x) = e^{i\eta\cdot x},\ u^1(x)n = -i\sqrt{\gamma_0}\,|\eta|\,e^{i\eta\cdot x},\ f(x,t) = e^{i\eta\cdot x - i\sqrt{\gamma_0}|\eta|t}.$$

Suppose that Γ_c and T geometrically control Ω; then we have

$$\begin{aligned}
&\int_0^T \int_{\Gamma_c} \left[\theta_\eta \left(\frac{\partial u_\alpha}{\partial n} - \frac{\partial u}{\partial n}\right) + \partial_t\theta_\eta \partial_t \left(\frac{\partial u_\alpha}{\partial n} - \frac{\partial u}{\partial n}\right)\right] \\
&= -\int_0^T \int_{\Gamma_c} e^{i\sqrt{\gamma_0}|\eta|t} \partial_t \left(e^{-i\sqrt{\gamma_0}|\eta|t} g_\eta\right) \left(\frac{\partial u_\alpha}{\partial n} - \frac{\partial u}{\partial n}\right) \qquad (5) \\
&= \alpha^d \sum_{j=1}^m \left(\frac{\gamma_0}{\gamma_j} - 1\right) e^{2i\eta\cdot z_j} \left[M_j(\eta)\cdot\eta - |\eta|^2 |B_j|\right] + o(\alpha^d) \quad \doteq \Lambda_\alpha(\eta),
\end{aligned}$$

where θ_η is the unique solution to the ODE (6)

$$\begin{cases} \partial_t\theta_\eta - \theta_\eta = e^{i\sqrt{\gamma_0}|\eta|t} \partial_t \left(e^{-i\sqrt{\gamma_0}|\eta|t} g_\eta\right) & \text{for } x \in \Gamma_c,\ t \in (0,T), \\ \theta_\eta(x,0) = \partial_t\theta_\eta(x,T) = 0 & \text{for } x \in \Gamma_c, \end{cases} \qquad (6)$$

with g_η the boundary control in (W_c), and M_j the polarization tensor of B_j.

Idea of the proof

- asymptotic formula for $\frac{\partial u_\alpha}{\partial \nu}$ on ∂B_j in terms of $\frac{\partial \Phi}{\partial \nu}$, $\frac{\gamma_0}{\gamma_j}$ and u;
- introduce auxilliary solution, v_α, of homogeneous wave equation with initial condition $\partial_t v_\alpha =$ the asymptotic principal term;
- show that the asymptotic equals the boundary average of $\frac{\partial v_\alpha}{\partial n} g_\eta$;
- finally, use θ_η and the Volterra equation (6) to replace v_α by u_α (using Taylor expansions and asymptotics in α)

Asymptotic formula

$$
\begin{aligned}
\Lambda_\alpha(\eta) &= -\int_0^T \int_{\Gamma_c} e^{i\sqrt{\gamma_0}|\eta|t}\partial_t\left(e^{-i\sqrt{\gamma_0}|\eta|t} g_\eta\right)\left(\frac{\partial u_\alpha}{\partial n} - \frac{\partial u}{\partial n}\right) \\
&\approx \alpha^d \sum_{j=1}^m \left(\frac{\gamma_0}{\gamma_j} - 1\right) e^{2i\eta\cdot z_j}\left[\boldsymbol{M}_j(\eta)\cdot\eta - |\eta|^2\left|\boldsymbol{B}_j\right|\right] \\
&\doteq \alpha^d \sum_{j=1}^m \boldsymbol{C}_j(\eta) e^{2i\eta\cdot z_j}.
\end{aligned}
$$

Asymptotic formula

$$\begin{aligned}
\Lambda_\alpha(\eta) &= -\int_0^T \int_{\Gamma_c} e^{i\sqrt{\gamma_0}|\eta|t}\partial_t \left(e^{-i\sqrt{\gamma_0}|\eta|t} g_\eta\right)\left(\frac{\partial u_\alpha}{\partial n} - \frac{\partial u}{\partial n}\right) \\
&\approx \alpha^d \sum_{j=1}^m \left(\frac{\gamma_0}{\gamma_j} - 1\right) e^{2i\eta\cdot z_j}\left[\boldsymbol{M}_j(\eta)\cdot\eta - |\eta|^2 \left|\boldsymbol{B}_j\right|\right] \\
&\doteq \alpha^d \sum_{j=1}^m \boldsymbol{C}_j(\eta) e^{2i\eta\cdot z_j}.
\end{aligned}$$

- Fundamental observation: the inverse Fourier transform gives a linear combination of (derivatives of) delta functions,

$$\Lambda_\alpha^{-1}(x) \approx \alpha^d \sum_{j=1}^m \boldsymbol{L}_j\left(\delta_{-2z_j}\right)(x)$$

Fourier algorithm

Reconsctruction Algorithm

- Sample values of $\Lambda_\alpha(\eta)$ at some discrete set of points and then calculate the corresponding discrete inverse Fourier transform.
- After a rescaling by $-\frac{1}{2}$, the support of this discrete inverse Fourier transform yields the location of the small imperfections B_α.
- Once the locations are known, we may calculate the polarization tensors $(M_j)_{j=1}^m$ by solving an appropriate linear system arising from (6). These polarization tensors give ideas on the orientation and relative size of the imperfections.

Other algorithms

By choosing other "currents", we can develop a variety of different methods:

- Kirchoff migration
- Back-propagation
- Arrival time
- MUSIC

Key references

H. Ammari, E. Bossy, V. Jugnon and H. Kang, *Mathematical Modelling in Photo-Acoustic Imaging.* SIAM Review **52**. (2010),
H. Ammari, M. Asch, V. Jugnon and H. Kang, *Transient wave imaging with limited-view data,* SIAM J. Imaging Sci., **4**, pp. 1097-1121 (2011).

Contents

Wave equation

- Standard $P_1 - Q_1$ finite element discretization in space.

$$\begin{cases} M U_h''(t) + K U_h(t) = B_h & 0 < t \leq T, \\ U_h(0) = U_h^0 \text{ and } U_h'(0) = V_h^0 \text{ given}, \end{cases} \tag{7}$$

- where,
  - mass matrix, M, has coefficients $M_{ij} = \int_\Omega \omega_i(x)\omega_j(x)dx$,
  - stiffness matrix, $K_{ij} = \int_\Omega \gamma(x)\nabla\omega_i(x)\nabla\omega_j(x)dx$,
  - and B_h is the right hand side vector.
- Newmark scheme in time (permits to pass from fully explicit to fully implicit schemes).

Bi-Grid HUM

- Newmark wave-equation solver.
- Bi-grid filter:
  - wave equations are solved on a fine mesh of size h
  - residuals are computed on a coarse mesh of size $2h$
- Conjugate gradient iteration for inversion of the HUM operator.

Key reference

A., G. Lebeau, *Geometrical aspects of exact boundary controllability for the wave equation a numerical study. ESAIM : Control, Optimisation and Calculus of Variations ; Vol.* ***3*** *; pp. 163-212 (1998).*

HUM simulations

- full-view on square and disc,
- partial-view on square and disc.

Fourier Imaging Algorithm

- Take a finite number of imperfections, $z_j + \alpha B_j$ for $j = 1, ..., m$, with conductivities γ_j.
- Then, for each $\eta \in [-\eta_m, \eta_m]^d$ in a discrete set D of values,
  1. Compute the solution u_α of the wave equation (W_α) by a finite element method to simulate the boundary data $\dfrac{\partial u_\alpha}{\partial n}$ on $\Gamma \times (0, T)$ for the inverse problem.
  2. Compute the quantity $\dfrac{\partial u}{\partial n}$ on $\Gamma_c \times (0, T)$ which is explicitly known from the initial conditions.
  3. Calculate the control g_η of (W_c) via the BiGrid HUM method.
  4. Form the quantity $\Lambda_\alpha(\eta)$ from the left hand side of (6) with a suitable quadrature formula.
- Finally, apply the inverse Fourier transform to $\Lambda_\alpha(\eta)$ (η in the Fourier space D) to compute $\check{\Lambda}_\alpha(x)$ (x in the physical space Ω).

Contents

Fourier calibration

Objective:

Recover Dirac masses situated at the points $-2z_j$ from the inverse transform of the asymptotic formula

$$\Lambda_\alpha(\eta) = \alpha^d \sum_{j=1}^{m} \left(\frac{\gamma_0}{\gamma_j} - 1 \right) e^{2i\eta \cdot z_j} \left[\boldsymbol{M}_j(\eta) \cdot \eta - |\eta|^2 \left| \boldsymbol{B}_j \right| \right], \quad d = 2, 3$$

Fourier calibration

Objective:

Recover Dirac masses situated at the points $-2z_j$ from the inverse transform of the asymptotic formula

$$\Lambda_\alpha(\eta) = \alpha^d \sum_{j=1}^{m} \left(\frac{\gamma_0}{\gamma_j} - 1 \right) e^{2i\eta \cdot z_j} \left[M_j(\eta) \cdot \eta - |\eta|^2 \left| B_j \right| \right], \quad d = 2, 3$$

- Numerous numerical issues arise:
  - resolution/cost -
  - aliasing/rippling -
  - instabilities for large $|\eta|$ -

Fourier calibration

Objective:

Recover Dirac masses situated at the points $-2z_j$ from the inverse transform of the asymptotic formula

$$\Lambda_\alpha(\eta) = \alpha^d \sum_{j=1}^{m} \left(\frac{\gamma_0}{\gamma_j} - 1 \right) e^{2i\eta \cdot z_j} \left[M_j(\eta) \cdot \eta - |\eta|^2 \left| B_j \right| \right], \quad d = 2, 3$$

- Numerous numerical issues arise:
  - resolution/cost - no free lunch... use parallel processing.
  - aliasing/rippling -
  - instabilities for large $|\eta|$ -

Fourier calibration

Objective:

Recover Dirac masses situated at the points $-2z_j$ from the inverse transform of the asymptotic formula

$$\Lambda_\alpha(\eta) = \alpha^d \sum_{j=1}^{m} \left(\frac{\gamma_0}{\gamma_j} - 1 \right) e^{2i\eta \cdot z_j} \left[M_j(\eta) \cdot \eta - |\eta|^2 \left| B_j \right| \right], \quad d = 2, 3$$

- Numerous numerical issues arise:
  - resolution/cost - no free lunch... use parallel processing.
  - aliasing/rippling - avoid truncation, respect periodicity of DFT.
  - instabilities for large $|\eta|$ -

Fourier calibration

Objective:

Recover Dirac masses situated at the points $-2z_j$ from the inverse transform of the asymptotic formula

$$\Lambda_\alpha(\eta) = \alpha^d \sum_{j=1}^{m} \left(\frac{\gamma_0}{\gamma_j} - 1 \right) e^{2i\eta \cdot z_j} \left[M_j(\eta) \cdot \eta - |\eta|^2 \left| B_j \right| \right], \quad d = 2, 3$$

- Numerous numerical issues arise:
  - resolution/cost - no free lunch... use parallel processing.
  - aliasing/rippling - avoid truncation, respect periodicity of DFT.
  - instabilities for large $|\eta|$ - use thresholding.

Example: Fourier resolution

thresholding and windowing

- Three imperfections: $z_1 = (0.63, 0.28)$, $z_2 = (0.39, 0.66)$, $z_3 = (0.73, 0.65)$, $\alpha = 0.03$, $\gamma_j = 10$.
- Sampling: $N = 256$, $\eta_m = 33$.

Example: Fourier resolution

thresholding and windowing

- Three imperfections: $z_1 = (0.63, 0.28)$, $z_2 = (0.39, 0.66)$, $z_3 = (0.73, 0.65)$, $\alpha = 0.03$, $\gamma_j = 10$.
- Sampling: $N = 256$, $\eta_m = 33$.

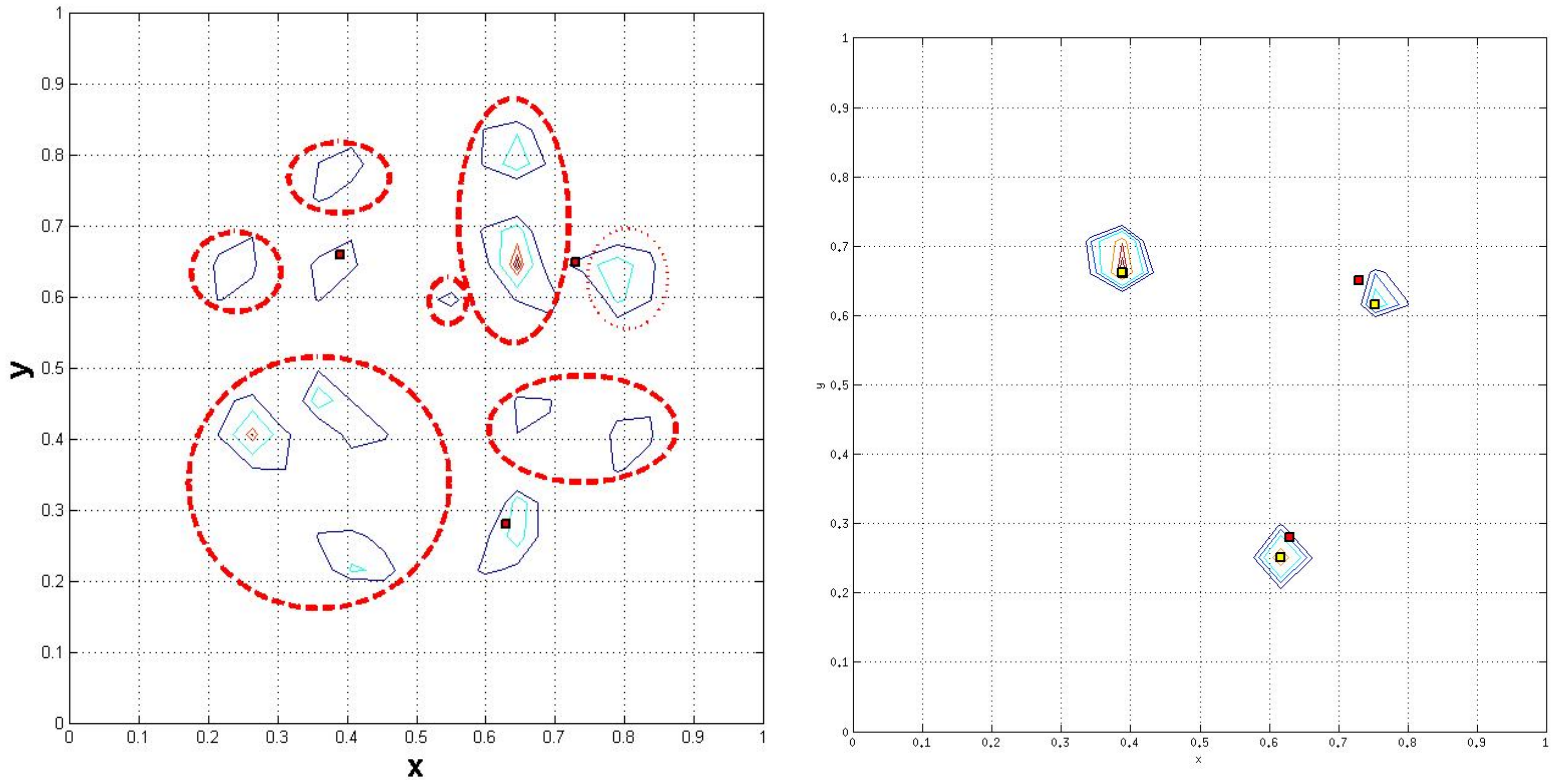

At left: without; at right: with thresholding (see [A., Mefire. IJNAM, **6** (1), 2009.])

Example: Transient imaging by Fourier in 3D

- Four imperfections centered at $z_1 = (0.66, 0.32, 0.47)$, $z_2 = (0.55, 0.71, 0.39)$, $z_3 = (0.39, 0.63, 0.31)$, $z_4 = (0.71, 0.42, 0.74)$.
- $N_e = 64$, $\eta_{\max} = 40$ and $\eta_* = 9$. Radius $\alpha = 0.01$ and conductivity $\gamma_j = 10$.

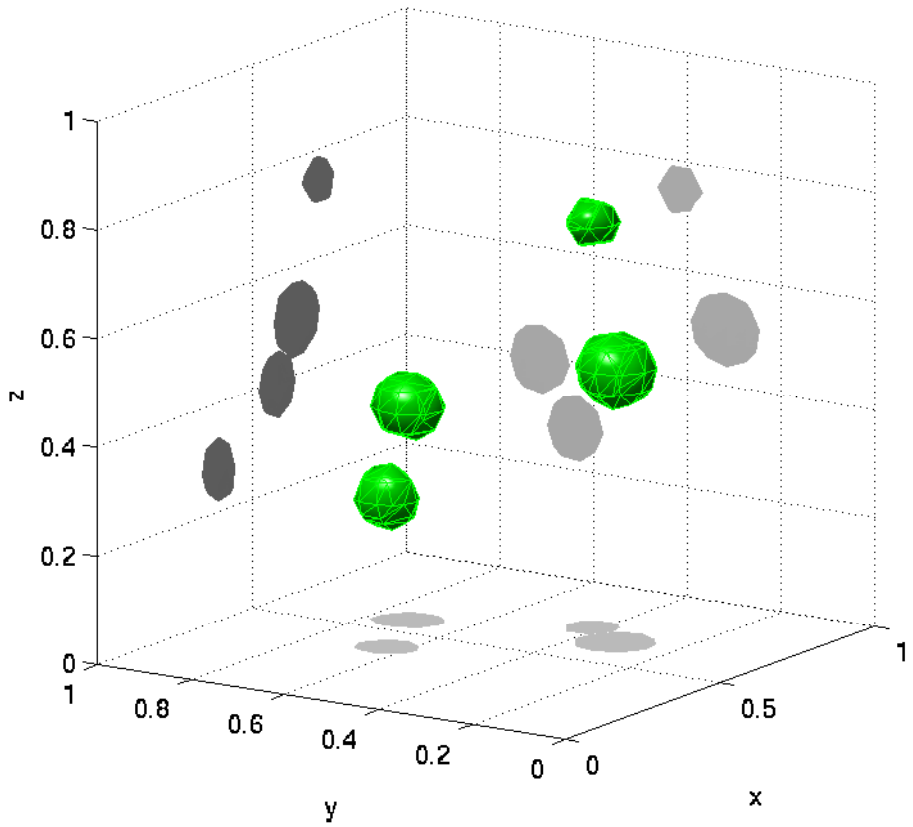

[A., Darbas, Duval. ESAIM-COCV, 2010.]

Limited-view data in 2- and 3D

- Repeat above computations, but compute measurements on a part of the bopundary that respects the geometric control condition (GCC)
- We obtain “perfect” reconstruction!

Limited-view data in 2- and 3D

- Repeat above computations, but compute measurements on a part of the bopundary that respects the geometric control condition (GCC)
- We obtain “perfect” reconstruction!

Conclusion:

As long as we can accurately compute the boundary control function, g, we can reconstruct equally well with limited-view data.

Some point source examples

here comes the MUSIC...

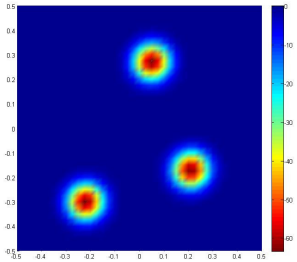

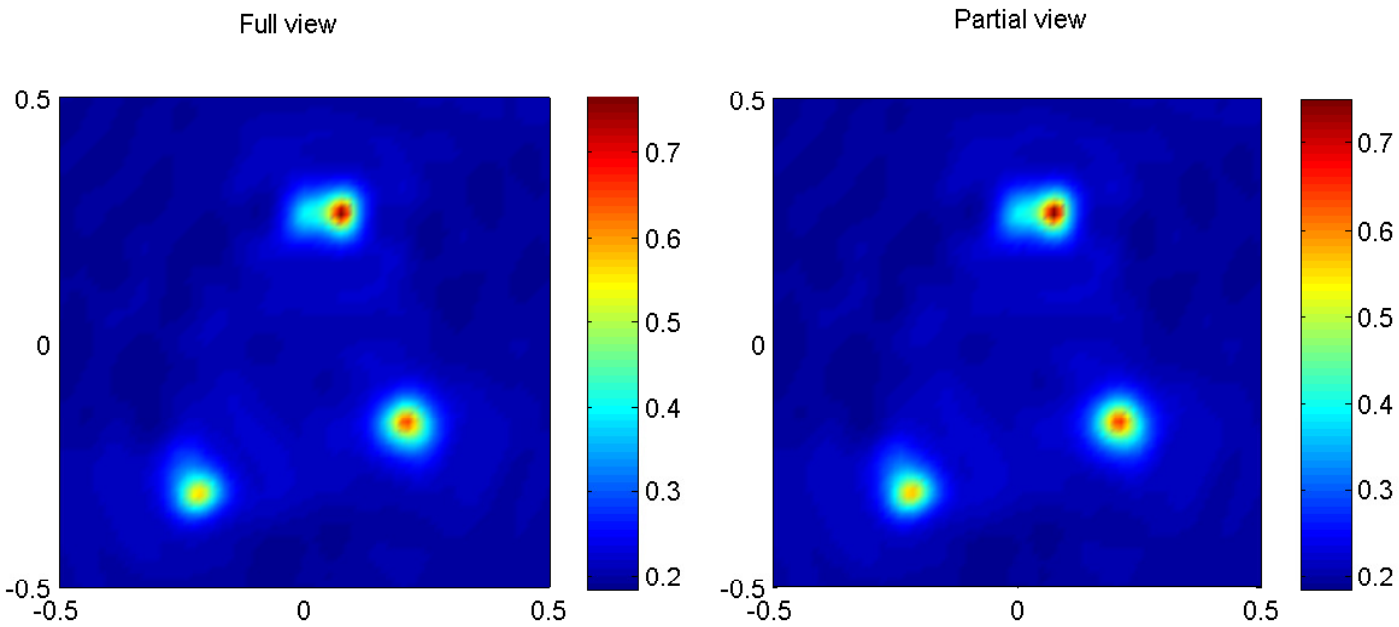

Computations performed by V. Jugnon

Contents

Contents

Replace:

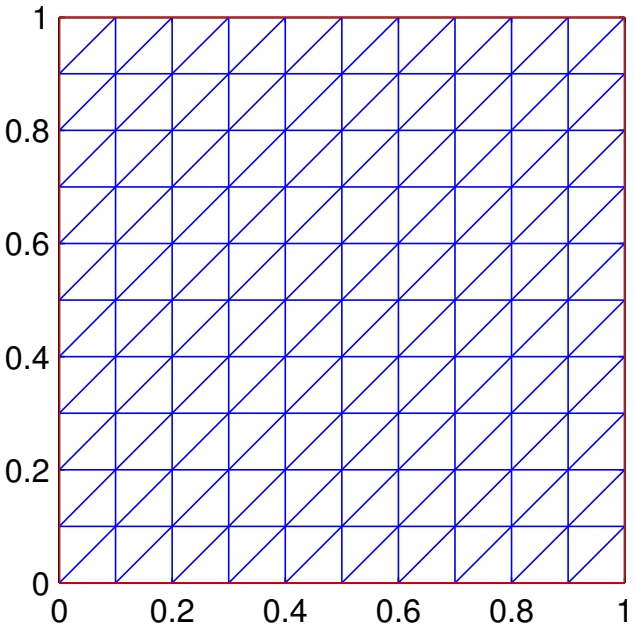

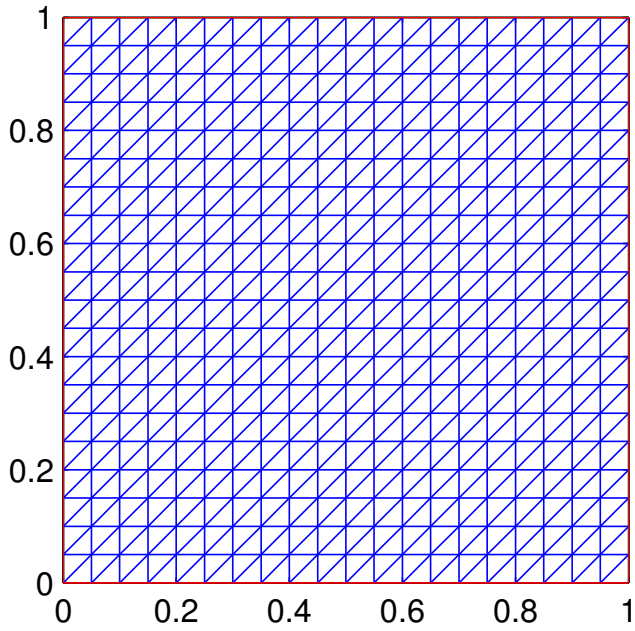

by:

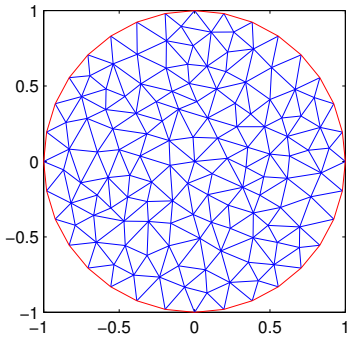
1
0.5
0
−0.5
−1
−1
−0.5
0
0.5
1

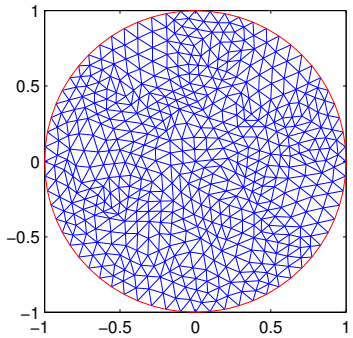
1
0.5
0
−0.5
−1
−1
−0.5
0
0.5
1

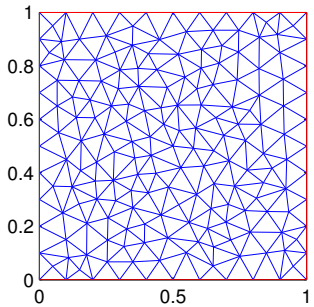
1
0.8
0.6
0.4
0.2
0
0
0.5
1

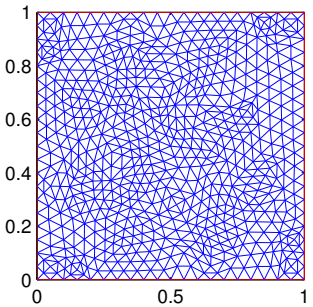
1
0.8
0.6
0.4
0.2
0
0
0.5
1

Contents

- Recall some classical FEM convergence results.

- Recall some classical FEM convergence results.
- Define mesh quality and its connection with FEM error.

- Recall some classical FEM convergence results.
- Define mesh quality and its connection with FEM error.
- How is all this related to BiGrid HUM?

- Recall some classical FEM convergence results.
- Define mesh quality and its connection with FEM error.
- How is all this related to BiGrid HUM?
- Preliminary numerical convergence results.

Convergence vs. mesh quality

- As seen previously, the convergence of the FEM depends on
  - mesh size
  - mesh quality
- Bi-grid HUM is strongly dependent on mesh quality because of the "brutal" nature of the filtering, $h \longrightarrow h/2$
- Error norms used for convergence of the HUM:
  - $\left\| u_0 - u_0^h \right\|_{L_2(\Omega)}$
  - $\left\| u(T) - u^h(T) \right\|_{L_2(\Omega)}$
  - other possibilities:
    - H^{-1}-norm of u_t;
    - L_2-norm of g (see A., Lebeau. ESAIM COCV'98)

(Preliminary) Numerical results

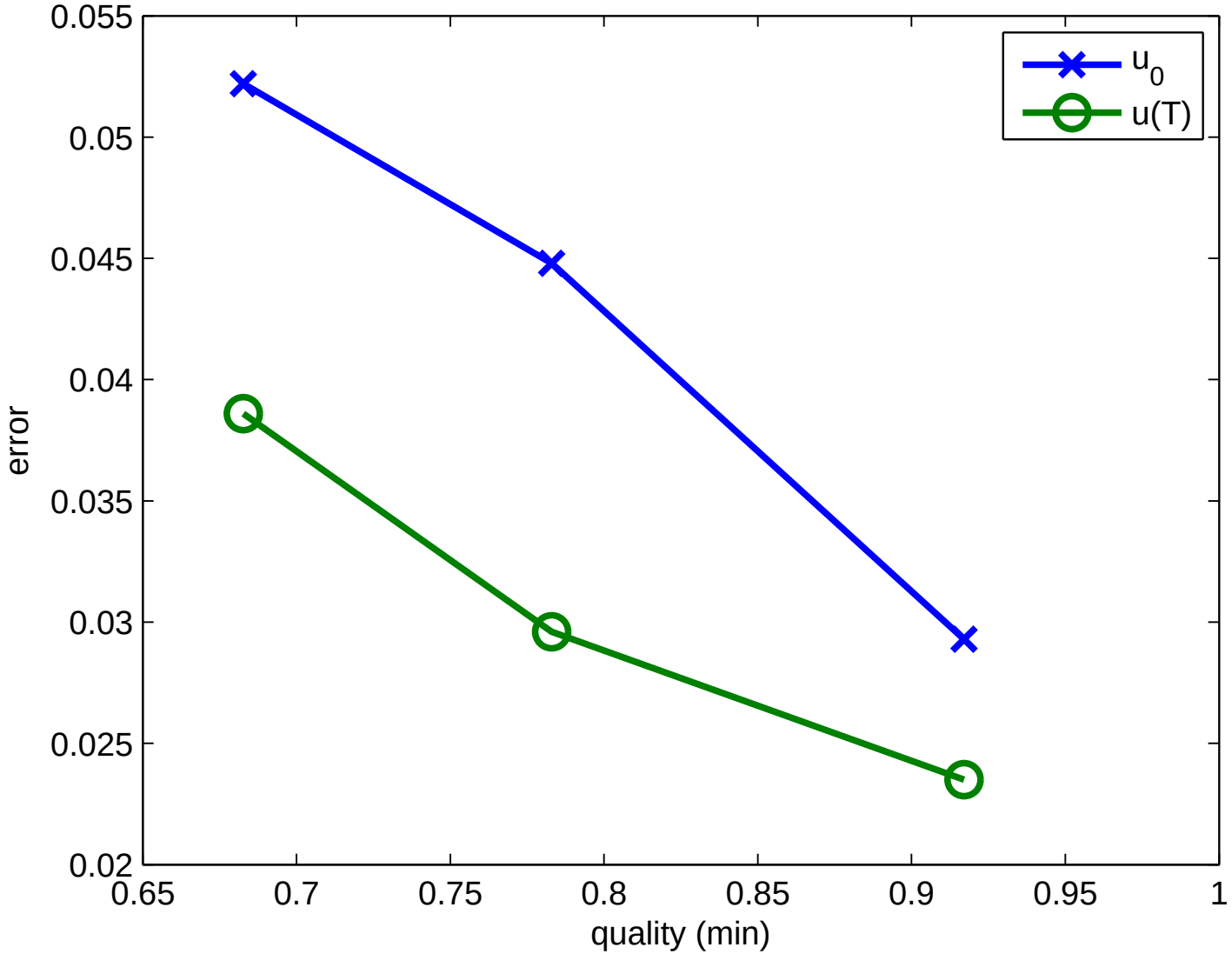

(Preliminary) Numerical results

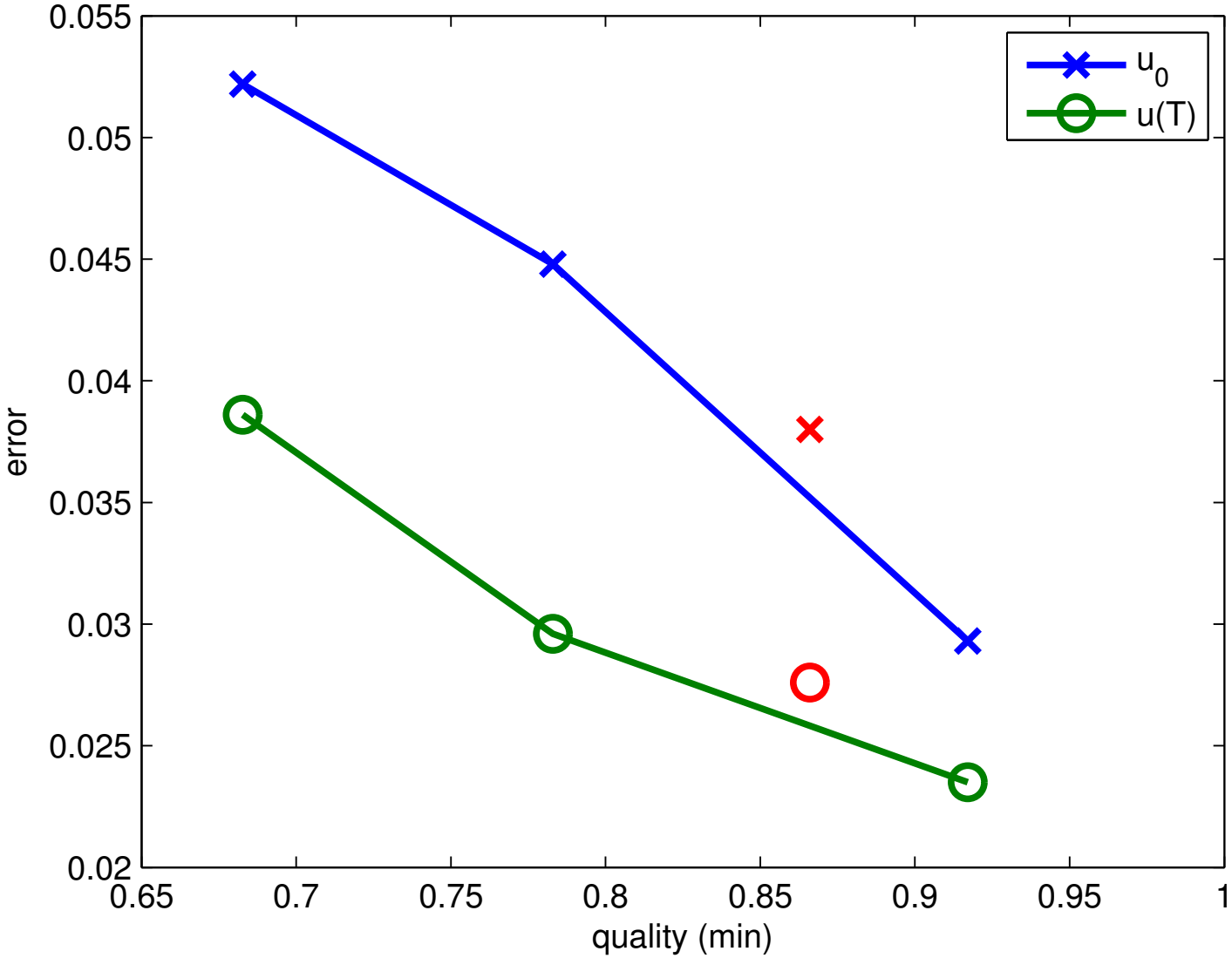

(Preliminary) Numerical results (contd.)

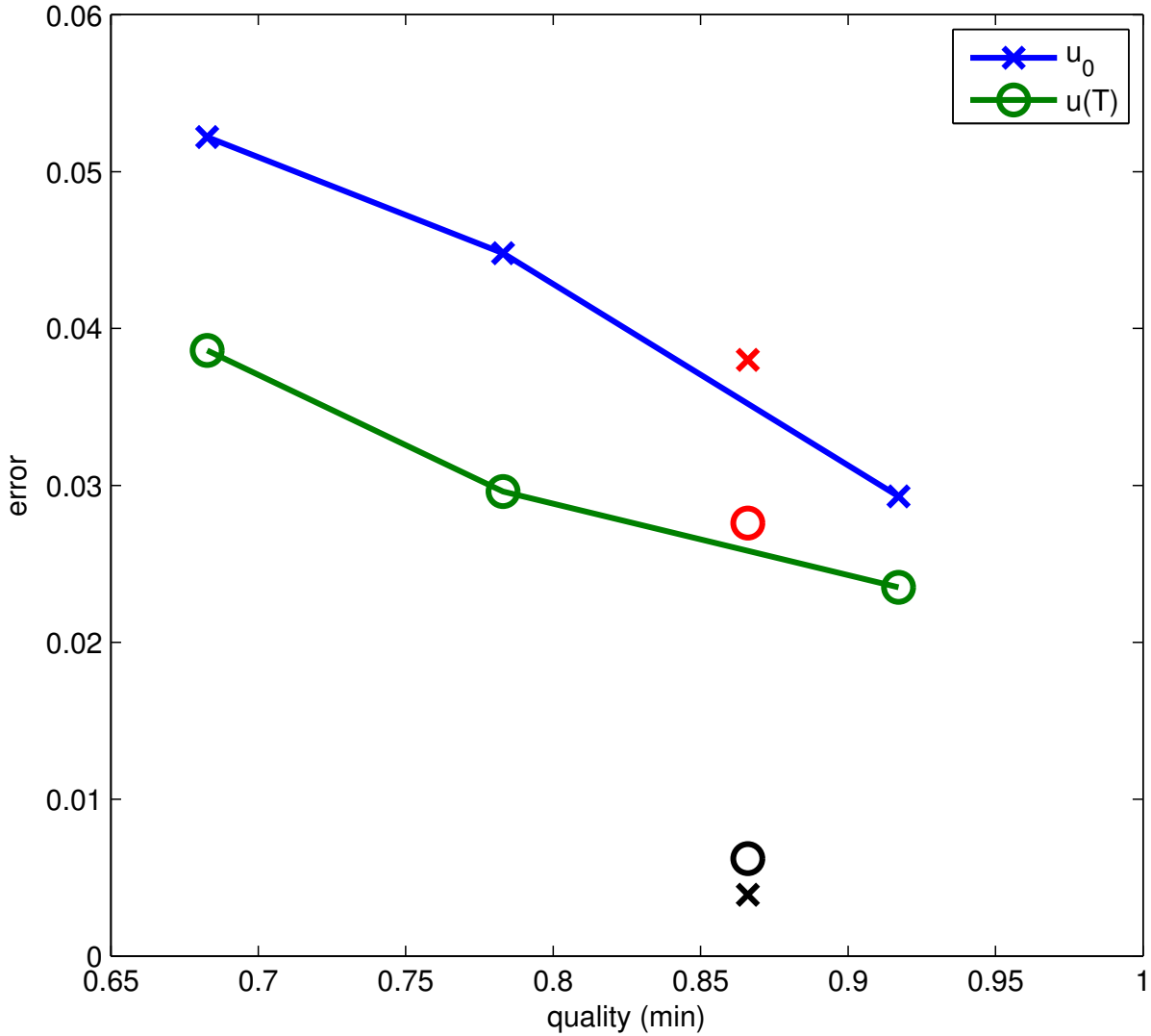

Contents

Conclusions

- Imaging:
  - Precise, robust and fast (non-iterative) imaging algorithms.
  - Can deal with limited-view data in a transient context.
- HUM:
  - Bi-grid performs well on unstructured meshes.
  - Optimizing the mesh quality improves the convergence.

Perspectives

- Imaging:
  - multi-wave imaging techniques (PAT, MAT, RFAT, etc.)
  - dissipative media which are far more realistic (especially for medical imaging)
  - random media...
- HUM:
  - general proof of Bi-grid convergence using FEM error estimates and mesh quality...

Thank you! Questions?

Further reading I


H. Ammari.
Asymptotic, multi-wave imaging... Consult
http:///www.cmap.polytechnique.fr/~ammari/


H. Ammari.
An Introduction to Mathematics of Emerging Biomedical Imaging. Mathématiques et Applications, Volume 62, Springer-Verlag, Berlin, 2008.


E. Zuazua.
HUM... Consult
http://www.bcamath.org/zuazua.